Article

RNA-Tethered Phenyl Azide Photocrosslinking via a Short-Lived Indiscriminant Electrophile

Karen L. Buchmueller, Brian T. Hill, Matthew S. Platz, and Kevin M. Weeks

J. Am. Chem. Soc., **2003**, 125 (36), 10850-10861• DOI: 10.1021/ja035743+ • Publication Date (Web): 16 August 2003

J|A|C|S
ARTICLES
Published on Web 08/16/2003

RNA-Tethered Phenyl Azide Photocrosslinking via a Short-Lived Indiscriminant Electrophile

Karen L. Buchmueller,[†] Brian T. Hill,[‡] Matthew S. Platz,*[,‡] and Kevin M. Weeks*[,†]

Contribution from the Department of Chemistry, University of North Carolina, Chapel Hill, North Carolina 27599-3290 and Chemistry Department, The Ohio State University, 100 West 18th Avenue, Columbus, Ohio 43210

Received April 22, 2003; E-mail: weeks@unc.edu; platz@chemistry.ohio-state.edu

Abstract: Arylazide mediated photocrosslinking has been widely used to obtain structural constraints in biological systems, even though the reactive species generated upon photolysis in aqueous solution have not been well characterized. We establish a mechanistic framework for formation of adducts between photoactivated 3-hydroxyphenyl azide and RNA. Tethered to an internal site in an RNA duplex via a 2′-amido linkage, photolysis of the aryl azide yields a cross-strand cross-link. Analysis of the ability of reagents with diagnostic reactivities to intercept formation of this cross-strand cross-link supports the assignment that the photoactivated intermediate is the ketenimine or a ketenimine-derived ring expansion product. Neither the initially produced singlet nitrene nor the subsequently formed triplet nitrene contribute to cross-link formation. Argon matrix and time-resolved solution experiments show that photolysis of free 3-hydroxyphenyl azide releases (in $\leq$20 ns) either a ketenimine or azepinone intermediate that reacts with nucleophiles. Adenosine, uridine, and guanosine monophosphate nucleotides have approximately equivalent abilities to quench the cross-strand cross-link, indicating that the photoactivated intermediate reacts broadly with functional groups in RNA. The reactive intermediate forms an adduct with adenosine monophosphate when tethered to both an RNA duplex or unstructured single strand; thus, cross-link formation is independent of the local RNA environment. The lifetime of the reactive intermediate generated upon photolysis of free 3-hydroxyphenyl azide in 50 mM Hepes diamine buffer is found to be 60−160 μs or significantly shorter than large scale RNA folding events. RNA-tethered 3-hydroxyphenyl azide cross-linking in aqueous buffer can thus be used with confidence to map structural neighbors, including most dynamic interactions, in RNA.

Introduction

Arylazide based photocrosslinking has been widely employed to obtain information on the higher order structure of RNA and RNA−protein complexes.[1,2] Following photoactivation of a tethered aryl azide, cross-linked products are typically resolved from non-cross-linked starting material as low mobility species using gel electrophoresis. Cross-linking partners can then be mapped by either selective degradation or primer extension of the RNA. Arylazide mediated cross-linking represents a potentially powerful approach for mapping RNA structural neighbors in three-dimensional space.

Despite widespread use, basic features of aryl azide chemistry in the context of an aqueous, roughly biological, environment have not been widely investigated. Two issues with significant implications for the quality of structural information obtainable by this chemistry are (i) the chemical selectivity of the reactive species and (ii) its lifetime. Ideally, the photogenerated intermediate should have broad, indiscriminant reactivity such that the photoactivated species is competent to react with most RNA structures. Second, the photoactivated species should have a short lifetime so that only RNA structures adjacent to the cross-linking moiety at the time of photolysis form covalent bonds.

In an example that illustrates the importance of these chemical issues, the structure of an RNA collapsed state has been recently investigated by photoinduced cross-linking.[3] Like many large RNAs, the catalytic core of the bI5 group I intron forms a conformationally collapsed, but not quite native, state prior to assembly with its obligate protein cofactor.[4,5] The structure of the bI5 catalytic core can be manipulated by varying the Mg^{2+} concentration and exists in the collapsed state at near-physiological Mg^{2+} concentrations (2−7 mM), sufficient to screen backbone charges. By careful selection of sites for derivatization with an internal phenyl azide group, 12 high quality intramolecular cross-links were obtained that report structural neighbors in the collapsed and native states and in an expanded state populated in the absence of Mg^{2+}.[3]

[†] University of North Carolina.
[‡] The Ohio State University.

(1) (a) Ofengand, J.; Schwartz, I.; Chinali, G.; Hixson, S. S.; Hixson, S. H. *Methods Enzymol.* **1977**, *46*, 683−702. (b) Burgin, A. B.; Pace, N. R. *EMBO J.* **1990**, *9*, 4111−4118. (c) Wang, J.-F.; Downs, W. D.; Cech, T. R. *Science* **1993**, *260*, 504−508. (d) Pinard, R.; Heckman, J. E.; Burke, J. M. *J. Mol. Biol.* **1999**, *287*, 239−251.
(2) Chen, J. L.; Nolan, J. M.; Harris, M. E.; Pace, N. R. *EMBO J.* **1998**, *17*, 1515−1525.
(3) Buchmueller, K. L.; Weeks, K. M. Submitted.
(4) Buchmueller, K. L.; Webb, A. E.; Richardson, D. A.; Weeks, K. M. *Nat. Struct. Biol.* **2000**, *7*, 362−366.
(5) Webb, A. E.; Weeks, K. M. *Nat. Struct. Biol.* **2001**, *8*, 135−140.

10.1021/ja035743+ CCC: $25.00

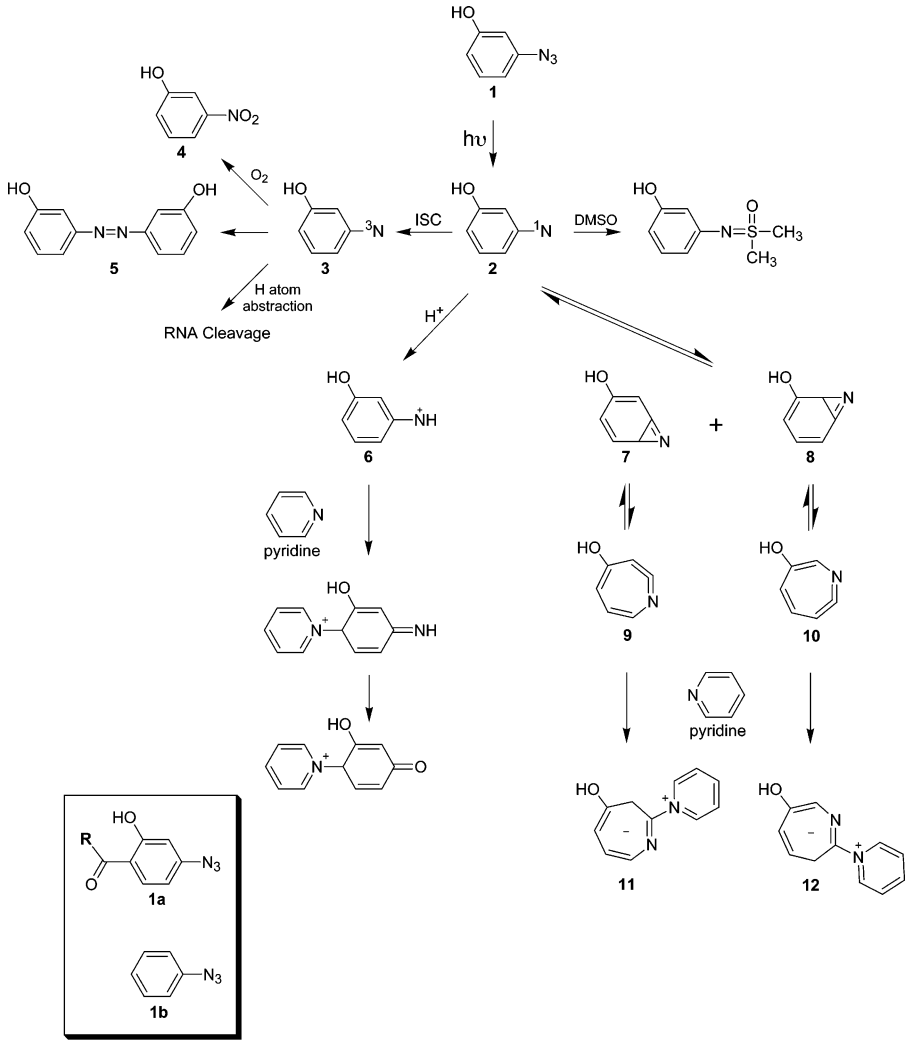

Figure 1. Potential reactive species produced upon photoactivation of an aryl azide.[6−9] (Inset) Structure of the RNA-tethered (R) 3-hydroxyphenyl azide (**1a**) used in the cross-linking experiments reported in this work and of the parent phenyl azide (**1b**). The specific product for reaction of a ketenimine (**9**/**10**) with pyridine in aqueous solution is not known; an approximate initial adduct is shown.

Strikingly, cross-linking patterns for the RNA native and collapsed states are essentially identical, even though only the native state folds to form a solvent inaccessible core.[3] The physical interpretation of the nearly indistinguishable cross-linking patterns for the collapsed and native states is dependent on the chemical selectivity and lifetime of the cross-linking species.

If the reactive cross-linking species shows significant chemical selectivity, then cross-linking partners will report the proximity of (potentially rare) reactive groups rather than true structural neighbors. If the lifetime of the reactive species were long relative to the time scale for RNA folding and rearrangement events, cross-linking might over report native-like structures relative to dynamic structural intermediates. Alternatively, if the photoactivated intermediate reacts broadly with RNA nucleotides and has a short lifetime, then the observed nearly identical cross-linking patterns in the bI5 RNA collapsed and native states[3] would strongly support the interpretation that these two states possess similar global structures.

To inform our own efforts in studying the ubiquitous, but inherently dynamic, bI5 RNA collapsed state[3−5] and to provide a framework for interpreting results from other studies, we have investigated the chemistry and lifetime of the reactive species produced in aqueous solution upon photolysis of the 3-hydroxyphenyl azide cross-linking group (structure **1** in Figure 1).

Potential Intermediates Produced upon Aryl azide Photolysis. Aryl azides and the cross-linking species produced by photolysis have been studied extensively, although largely in nonaqueous environments (reviewed in refs 6−9). Four reactive intermediates, the singlet nitrene (**2**),[8] triplet nitrene (**3**),[8] ketenimine (**9**/**10**),[10,11] and nitrenium ion (**6**),[9,12] resulting from photolysis of phenyl azide (**1** or **1b**), have been identified (Figure 1). In any single system, one or more of these intermediates may be present. Substitution of the aromatic ring,[11,13−16] solvent conditions,[13,17] temperature,[18] aryl azide concentration,[11,19] and

(6) Iddon, B.; Meth-Cohn, C.; Scriven, E. F. V.; Suschitzky, H.; Gallagher, P. T. *Angew. Chem., Int. Ed. Engl.* **1979**, *18*, 900−917.
(7) Smith, P. A. S. In *Azides and Nitrenes, Reactivity and Utility*; Scriven, E. F. V., Ed.; Academic Press: 1984; pp 95−204.
(8) Schuster, G. B.; Platz, M. S. *Adv. Photochem.* **1992**, *17*, 69−143.
(9) McClelland, R. A.; Gadosy, T. A.; Ren, D. *Can. J. Chem.* **1998**, *76*, 1327−1337.
(10) Chapman, O. L.; LeRoux, J.-P. *J. Am. Chem. Soc.* **1978**, *100*, 282−285.
(11) Li, Y.-Z.; Kirby, J. P.; George, M. W.; Poliakoff, M.; Schuster, G. M. *J. Am. Chem. Soc.* **1988**, *110*, 8092−8098.
(12) Ren, D.; McClelland, R. A. *Can. J. Chem.* **1998**, *76*, 78−84.
(13) Schnapp, K. A.; Poe, R.; Leyva, E.; Soundararajan, N.; Platz, M. S. *Bioconjugate Chem.* **1993**, *4*, 172−177.
(14) Schnapp, K. A.; Platz, M. S. *Bioconjugate Chem.* **1993**, *4*, 178−183.

Scheme 1

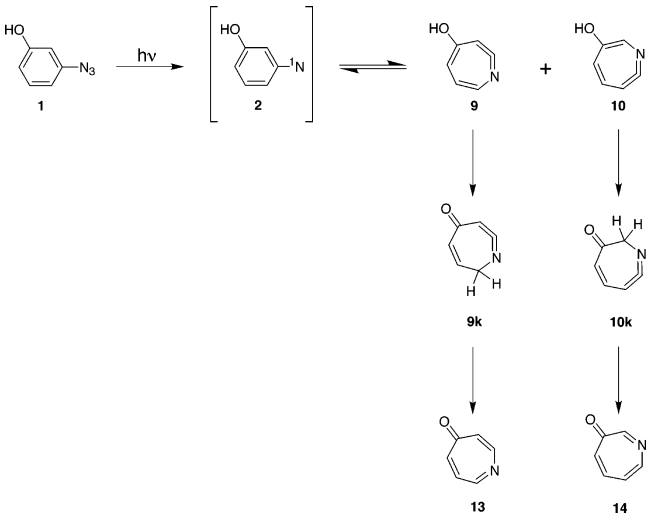

light source intensity[19] can contribute to the relative yields and reactivity of the potential reactive intermediates.

Photoactivation of an aryl azide (**1** or **1b**) initially produces the corresponding singlet nitrene (**2**).[8] Long-lived singlet nitrenes bearing electron accepting substituents can react with sulfoxides or add to C=C bonds to form aziridines,[17,20] (Figure 1) but this chemistry is not likely for the nitrene generated in this work.[20] Singlet nitrenes (**2**) with carbonyl substituents in the *para* position have lifetimes of ~1 ns at ambient temperature[8,11] controlled by rearrangement to benzazirines (**7**/**8**) and ketenimines (**9**/**10**). The singlet nitrene can also undergo intersystem crossing to the triplet. This process becomes favored as the temperature is lowered. Triplet nitrenes (**3**) can react (i) with O_2 to eventually form the corresponding nitrobenzene (**4**),[8] (ii) with a second triplet nitrene *or* with an azide precursor to form an azo dimer (**5**),[8] (iii) via electron abstraction from reducing agents, or (iv) via hydrogen-atom abstraction,[6] with the potential to cause RNA backbone cleavage (Figure 1). Triplet nitrene lifetimes in water are long, ≥1 ms.[21]

Alternatively, the initially formed singlet nitrene can react with a proton donor to form a nitrenium ion[22] (**6**) or isomerize to form the ketenimine (**9**/**10**) (Figure 1) via a benzazirine intermediate. Photolysis of aryl azides with hydroxy substituents will form hydroxy-substituted ketenimines which may isomerize to the azepinone (**13**/**14**, Scheme 1). Nitrenium ion, ketenimine, and azepinone species react with nucleophiles. The ketenimine is expected to react with nitrogenous nucleophiles such as diethylamine or pyridine to form 3*H* azepines (**11**/**12**)[7,11,14] (Figure 1), with rate constants of 10^5-10^6 M^{-1} s^{-1}. Reaction of ketenimines with alcohols and water is rare.[8,20] Ketenimine lifetimes in heptane, corrected for quenching of the ketenimine by unreacted azide starting material, are quite long at 5 ms.[11] Nitrenium ions react with nucleophiles with larger rate constants than do ketenimines and exhibit a strong reaction selectivity for guanine over other nucleoside bases.[9] Nitrenium ion lifetimes in water are microseconds or less, depending on ring substituents.[12,23] Azepinone reactivity[16,24] with nucleophiles is relatively unexplored but plausibly involves Michael-like addition chemistry.

We study single stranded and duplex RNA structures (Figure 2B and C), incorporating a unique 3-hydroxyphenyl azide group at an internal position (Figure 2A), to investigate the nature of the RNA-tethered reactive species. In the absence of added quenching agents, photolysis of the aryl-azide-derivatized duplex yields a single, predominant, cross-strand cross-link (Figure 2C and D).[3] Reagents with diagnostic chemical reactivities were then tested for their ability to quench formation of this cross-link. Our results are consistent with RNA cross-linking via a ketenimine-derived electrophile that reacts broadly with Hepes buffer, pyridine, and nucleotide monophosphates. Second, the photochemistry of free 3-hydroxyphenyl azide was investigated by time-resolved spectroscopy. The lifetime of the photogenerated ketenimine-derived species is 60−160 μs in our aqueous buffer system.

Results

Cross-Linking by a Tethered Phenyl Azide in an RNA Duplex. A 3-hydroxy-substituted phenyl azide was chosen for RNA cross-linking studies because the hydroxyl group shifts the spectrum to longer wavelengths, where RNA does not absorb. The 3-hydroxy group may also advantageously shorten the lifetime of the reactive species.[6,8,11] 3-Hydroxy-4-carboxyphenyl azide (**1a**) has two absorption peaks, a main peak at 283 nm and a shoulder at ~315 nm (extinction coefficients 19 and 10 mM^{-1} cm^{-1}, respectively; Figure 3A). RNA bases absorb light below 300 nm (λ_{max} 260 nm) leading to a reaction that can produce RNA−RNA cross-links and also cause RNA strand scission. Thus, the 3-hydroxyphenyl azide group was photolyzed using polystyrene-filtered UV light. Irradiation wavelengths and the polystyrene filter profile are shown with a gray bar and dashed line, respectively, in Figure 3A.

UV irradiation of the 84D duplex RNA (Figure 2C) yields a slowly migrating band as resolved by denaturing gel electrophoresis. The UV-induced band reflects formation of a covalent bond between the ^{32}P-labeled phenyl-azide-derivatized and the complementary strands in the duplex (Figure 3B). The cross-linking partner was mapped by alkaline hydrolysis of gel purified cross-linked RNA[3] and lies immediately across from the aryl azide in the duplex (Figure 2D). After 10 min of steady-state irradiation, formation of the cross-strand cross-link is saturated at ~7% (Figure 3C). A 1 min irradiation period yields ~30% of the cross-link intensity observed at saturation and was chosen as the standard irradiation time for subsequent work designed to explore the chemical selectivity of the photoactivated species.

Reactive Intermediate Does Not React with Sulfoxide or Acrylamide: Evidence Against the Singlet Nitrene. The

(15) (a) Gritsan, N. P.; Tigelaar, D.; Platz, M. S. *J. Phys. Chem.* **1999**, *103*, 4465−4469. (b) Gritsan, N. P.; Gudmundsdottir, A. D.; Tigelaar, D.; Zhu, Z.; Karney, W. L.; Hadad, C. M.; Platz, M. S. *J. Am. Chem. Soc.* **2001**, *123*, 1951−1962.
(16) Dunkin, I. R.; Ayeb, A. A.; Gallivan, S. L.; Lynch, M. A. *J. Chem. Soc., Perkin Trans. 2* **1997**, 1419−1427.
(17) Poe, R.; Schnapp, K.; Young, M. J. T.; Grayzar, J.; Platz, M. S. *J. Am. Chem. Soc.* **1992**, *114*, 5054−5067.
(18) Leyva, E.; Platz, M. S.; Persey, G.; Wirz, J. *J. Am. Chem. Soc.* **1986**, *108*, 3783−3790.
(19) Schrock, A. K.; Schuster, G. B. *J. Am. Chem. Soc.* **1984**, *106*, 5228−5234.
(20) Gritsan, N. P.; Platz, M. S. *Adv. Phys. Org. Chem.* **2001**, *36*, 255−304.
(21) Chen, T.; Michalak, J.; Platz, M. S. *Photochem. Photobiol.* **1995**, *61*, 600−606.
(22) McClelland, R. A.; Kahley, M. J.; Davidse, P. A.; Hadzialic, G. *J. Am. Chem. Soc.* **1996**, *118*, 4794−4803.
(23) Ramlall, P.; Li, Y.; McClelland, R. A. *J. Chem. Soc., Perkin Trans.* **1999**, *2*, 1601−1607.
(24) Proctor, G. R.; Redpath, J. In *Monocyclic Azepines: The Syntheses and Chemical Properties of the Monocyclic Azepines*; Wiley-Interscience: 1996; pp 592−606.

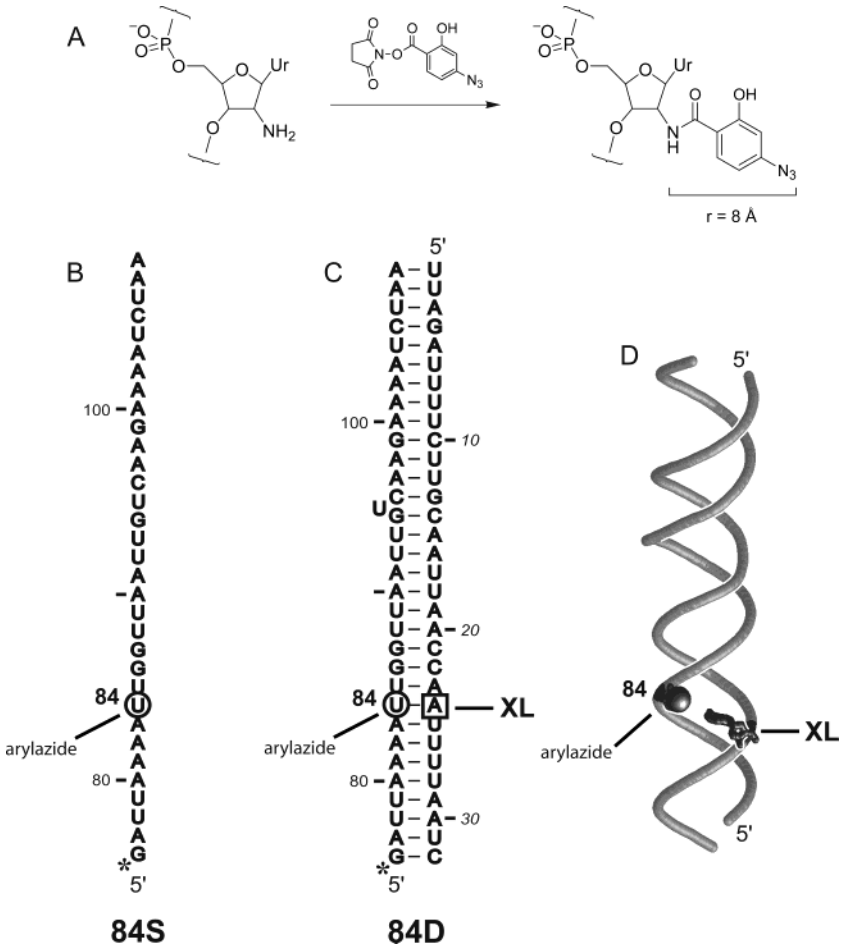

Figure 2. RNA constructs for phenyl azide cross-linking analysis. (A) Site-specific incorporation of 3-hydroxyphenyl azide into RNA via a unique 2′-amine-substituted nucleotide. (B,C) 33 nt single stranded (84S) and 32 base pair duplex (84D) RNAs. Position of the 5′-[^{32}P] radiolabel is shown with an asterisk. The aryl-azide-derivatized strand is numbered relative to the parent sequence in the bI5 group I intron RNA.[3] Upon UV irradiation of the 84D RNA, a single predominant cross-link (XL) is formed with nucleotide 24 in the complementary strand,[3] as visualized in three dimensions in part D.

singlet nitrene (**2**) is expected to exhibit a broad and relatively indiscriminant reactivity, and sufficiently long-lived nitrenes will, for example, react with sulfoxides and insert into C═C bonds.[17] Two water soluble organic reagents, acrylamide and dimethyl sulfoxide (DMSO), were therefore tested for their ability to compete with formation of the 84D duplex cross-link.

Cross-linking efficiency was not affected by the presence of 5.2 M acrylamide (see acrylamide lane in Figure 4A). Similarly, when the concentration of DMSO is increased in 10% (v/v, 1.4 M) increments, no change in cross-linking intensity is observed until complete quenching of the cross-link at 8.4 M DMSO. The sharp transition at high molar DMSO concentration suggests that interference with cross-linking is indirect and reflects RNA denaturation by the organic cosolvent. Therefore, neither DMSO nor acrylamide compete with formation of the cross-strand duplex cross-link at concentrations up to 5 M. Although the singlet nitrene is the first product of photolysis (Figure 1), it decays too rapidly[17] to contribute to cross-link formation.

Reactive Intermediate Does Not Yield Duplex Dimers: Evidence Against a Triplet Nitrene. Of the several products expected for reaction of the triplet nitrene (**3**), only formation of azobenzene dimers (**5**) would yield an apparent cross-link (see Figure 1). In contrast, hydrogen atom abstraction might induce RNA backbone cleavage but would not yield a cross-link. Similarly, formation of the nitrobenzene (**4**) would quench the triplet reactive species and also not result in a covalent cross-link. We find that the observed pattern of cross-linking (Figure 3B) is unchanged for duplex cross-linking reactions performed at concentrations ranging from 0.4 to 850 nM RNA (data not shown). The absence of a detectable concentration dependence rules out a contribution to cross-linking via formation of a bimolecular azobenzene (**5**) triplet product. In addition, cross-linking is unaffected when 80% (v/v) of the reaction volume was replaced by nitrogen saturated water (data not shown). Oxygen is an efficient scavenger of triplet nitrenes,[8,20] and radical and triplet lifetimes decrease by an order of magnitude or more[18,25] for nitrogen purged versus air saturated solutions. The absence of any detectable oxygen-mediated quenching of cross-linking, via nitrobenzene (**4**) formation, provides additional support for the lack of triplet involvement in cross-link formation.

Photoactivated Intermediate Reacts with the Pyridine Nucleophile. The intensity of the duplex cross-link decreased in the presence of modest concentrations of pyridine (Figure 4B). Half-maximal quenching ($Q_{1/2}$) occurs at 14 mM (Figure 4C). We tested whether pyridine reacts directly with 3-hydroxyphenyl azide in the dark or selectively quenches a UV-activated species. The 84D duplex RNA was incubated with pyridine for 2 or 10 min, prior to the 1 min photolysis period (right most lanes in Figure 4B). If pyridine reacts directly with the

(25) Liang, T.-Y.; Schuster, G. B. *J. Am. Chem. Soc.* **1987**, *109*, 7803−7810.

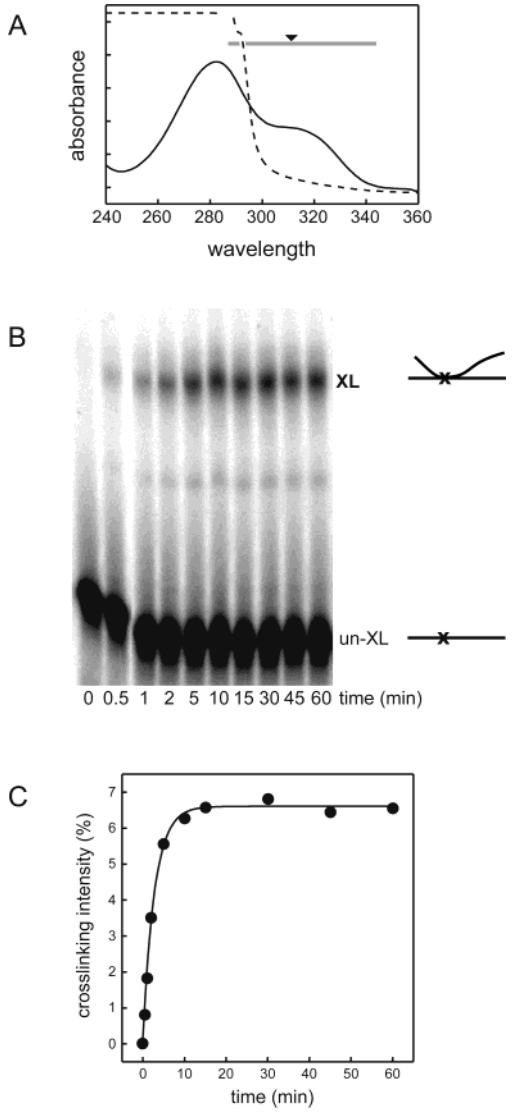

Figure 3. 3-Hydroxyphenyl azide cross-linking with the 84D duplex. (A) Absorption spectrum of 4-carboxy-3-hydroxyphenyl azide. UV irradiation wavelengths (285−345 nm) and λ_{max} (312 nm) are shown with a gray bar and triangle, respectively. Short wavelength light was suppressed using a polystyrene filter. Absorbance spectrum of filter in arbitrary units is shown with a dashed line. (B) Formation of the 84D cross-link (XL) as a function of steady-state irradiation time, visualized by denaturing gel electrophoresis. Position of phenyl azide group is shown with an ×. (C) Maximum cross-link intensity (7%) is reached at ∼10 min and is 30% saturated at 1 min.

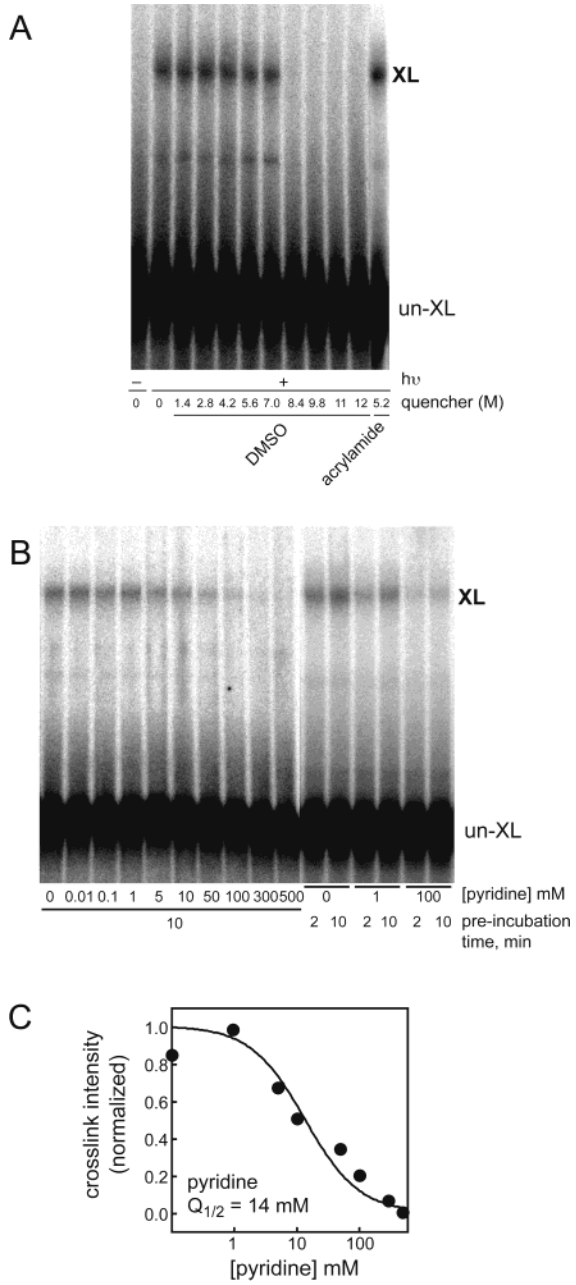

Figure 4. Chemical reactivity of the photoactivated cross-linking species. (A) DMSO and acrylamide do not quench formation of the 3-hydroxyphenyl-azide-mediated cross-link (XL) at nondenaturing concentrations. 84D RNA was incubated in the presence of DMSO or acrylamide and subjected to UV-irradiation (+*hυ*). Only the largest concentration of acrylamide tested is shown. (B) Quenching of the 84D duplex cross-link (XL) with pyridine. Right most lanes illustrate quenching as a function of preincubation time, prior to photolysis. (C) Determination of the pyridine concentration midpoint, $Q_{1/2}$, required to reduce cross-link intensity by one-half. Curve represents a best fit to intensity = $Q_{1/2}/(Q_{1/2}$ + [pyridine]).

unactivated azido group on the minute time scale, then the longer preincubation time would result in greater quenching of the duplex cross-link. Instead, no significant difference in quenching is observed for preincubation of pyridine with the phenyl azide-derivatized duplex RNA (Figure 4B). These data support the interpretation that the pyridine nucleophile reacts only with the photoactivated species.

Both the ketenimine (**9**/**10**) and nitrenium ion (**6**) are known to react with nucleophiles such as pyridine.[7−9] Ketenimine versus nitrenium ion pathways can be distinguished based on their reactivities with nucleotides because the nitrenium ion shows a strong kinetic preference (100−1000-fold) for reaction with guanine.[9] In addition, nitrenium ions, but not ketenimines, react with halides at diffusion controlled rates.[9,22]

Reactivity of the 84D RNA with Nucleotide 5′-Monophosphates: Evidence for a Reactive Ketenimine or Ketenimine-Derived Species. We have previously observed that addition of simple ions can decrease the efficiency of formation of the 84D duplex cross-link.[3] Quenching likely reflects an indirect effect due to greater rigidity of the RNA helix with increasing cation concentrations.[26] To provide a baseline for ionic strength effects on cross-link efficiency, we evaluated the ability of buffered sodium phosphate, as a model for the ionic component

(26) (a) Kebbekus, P.; Draper, D. E.; Hagerman, P. J. *Biochemistry* **1995**, *34*, 4354−4357. (b) Steger, G.; Muller, H.; Riesner, D. *Biochim. Biophys. Acta* **1980**, *606*, 274−284.

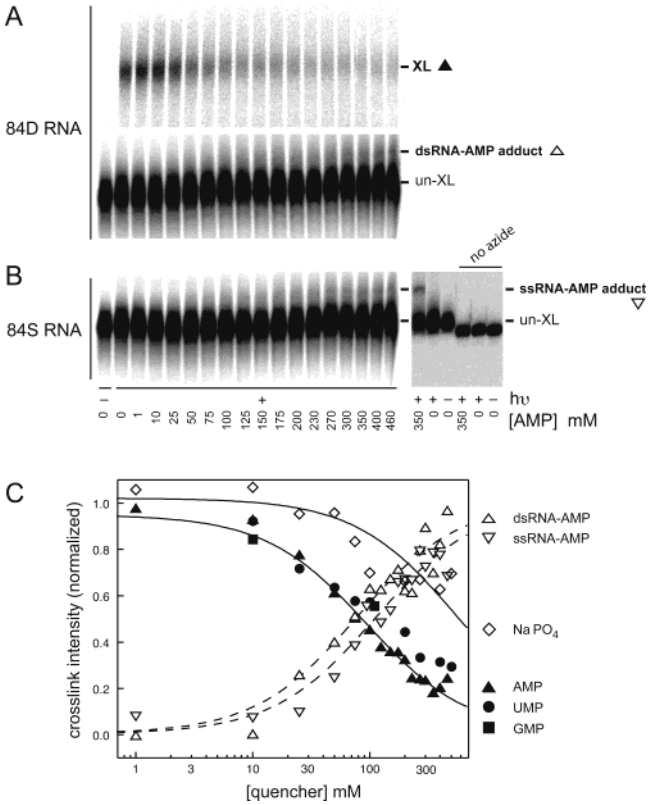

Figure 5. Quenching and adduct formation by nucleotide 5′-monophosphates and sodium phosphate. (A) Quenching of the cross-strand duplex cross-link by AMP (upper panel) and visualization of AMP adducts with the 84D double stranded RNA (lower panel). For clarity, the lower panel is shown at reduced exposure compared to the upper panel. (B) Formation of an adduct between AMP and the 84S single stranded RNA. For the right-hand panel, the irradiation time was 10 min. (C) Quantification of competition for the duplex cross-link and of formation of AMP adducts. $Q_{1/2}$ values for quenching by AMP and UMP are 90 and 130 mM and for formation of duplex-AMP, and single stranded-AMP adducts are 80 and 110 mM, respectively. $Q_{1/2}$ for sodium phosphate is greater than 600 mM.

of a nucleotide monophosphate, to quench the duplex cross-link. Sodium phosphate is a poor quencher: at 500 mM, the duplex cross-link still forms with 60% of the efficiency observed in the absence of this quencher (see open diamonds, Figure 5C). We conclude that phosphate and sodium ions only inefficiently quench the RNA-tethered phenyl azide.

Adenosine, uridine, and guanosine 5′-monophosphates each quench the duplex cross-link. Representative data for AMP are shown in Figure 5A. The concentrations of AMP and UMP required to quench the cross-link by one-half are similar at 90 and 130 mM, respectively (Figure 5C). Although the GMP concentration was limited to 100 mM, it is clear that the quenching profile for GMP is similar to, and certainly not significantly more efficient than, that of AMP and UMP (compare filled symbols in Figure 5C). Similar quenching profiles for AMP, UMP, and GMP are also consistent with the observation that phenyl-azide-mediated cross-linking yields efficient adducts to all four ribonucleotides for both the RNase P[2] and bI5[3] RNAs. Moreover, similar quenching profiles for AMP, UMP, and GMP rule out reaction via a nitrenium ion intermediate, because the nitrenium ion reacts preferentially with guanine.[9]

AMP Adducts with RNA-Tethered 3-Hydroxyphenyl Azide. For quenching experiments performed with the 84D duplex and 84S single stranded RNAs in the presence of AMP, a cross-linking product was detected that migrates slightly slower than the un-cross-linked RNA (Figure 5A, lower panel, and B). Formation of this band requires UV irradiation, AMP, and the presence of the phenyl azide in the 84S RNA (right panel in Figure 5B). The photoproduct therefore involves specific adduct formation between a 3-hydroxyphenyl-azide-derived species and AMP and not photoactivation of AMP directly. Formation of the dsRNA−AMP adduct exactly parallels (in reverse) quenching of the cross-strand duplex cross-link by AMP (compare upper and lower panels in Figure 5A). Transition midpoints for loss of the duplex cross-link and formation of the AMP adduct are identical within error at 90 and 80 mM, respectively (see open and closed triangles in Figure 5C). Thus, AMP directly competes with cross-linking by forming an adduct in place of the cross-strand cross-link.

When cross-linking experiments are performed with the single stranded 84S RNA in the absence of any quencher, no *intra*molecular cross-linking products are resolved as either slowly or rapidly[27] migrating bands (see no AMP lanes in Figure 5B and data not shown). The persistence length of an unstructured single stranded RNA is likely to be roughly similar to that of single stranded DNA, at approximately six nucleotides.[28] This effective length is much longer than that of the tethered 3-hydroxyphenyl azide group (8 Å, Figure 2A). The absence of a detectable lariat cross-link with the 84S single stranded RNA emphasizes that an RNA structure must be proximal to the photoactivated group in order to form a cross-link. However, irradiation of the 84S RNA in the presence of AMP yields an RNA−AMP adduct (Figure 5B), whose mobility is identical to that observed for the 84D duplex RNA. The $Q_{1/2}$ (=110 mM) for formation of the adduct is also similar to that observed for the duplex RNA (compare open triangles and inverted triangles in Figure 5C).

Thus, the single stranded 84S phenyl-azide-derivatized RNA is competent for cross-linking, but the lack of intramolecular cross-linking emphasizes the high structural specificity of this photo-cross-linking approach. Moreover, because the transition midpoints for AMP adduct formation with the 84D duplex and unstructured 84S RNAs are similar (dashed lines in Figure 5C), reactivity of the photogenerated intermediate is independent of the local RNA environment to which 3-hydroxyphenyl azide is tethered.

Visualizing Pyridine, Hepes, and Nucleotide Monophosphate Nucleophile Adducts. Pyridine and UMP also intercept the cross-strand cross-link, and therefore, we sought to visualize directly adducts between these reagents and the 84S RNA. In addition, the Hepes [4-(2-hydroxyethyl)-1-piperazineethanesulfonic acid] buffer used in our experiments is a functionalized piperazine diamine and might also form direct adducts with a ketenimine (**9**/**10**, Figure 1) or ketenimine-derived (Scheme 1) electrophile.

We visualized these additional low molecular mass adducts with the 84S RNA by resolving photolysis products by electrophoresis over 32−34 cm in a long denaturing gel (Figure 6). The aryl-azide-derivatized RNA migrates slightly more slowly than the unmodified 2′-amine-substituted RNA (compare lanes 1 and 3 in Figure 6). In our standard Hepes/KCl buffer,

(27) Williamson, J. R.; Raghuraman, M. K.; Cech, T. R. *Cell* **1989**, *59*, 871−880.
(28) Mills, J. B.; Vacano, E.; Hagerman, P. J. *J. Mol. Biol.* **1999**, *285*, 245−257.

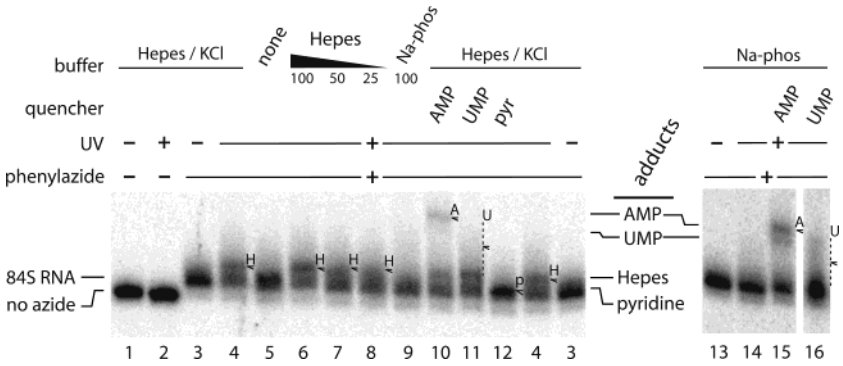

Figure 6. Visualization of adducts formed upon photolysis of RNA-tethered 3-hydroxyphenyl azide by denaturing electrophoresis. Adducts with *H*epes, *A*MP, *U*MP, or *p*yridine are indicated with small arrows and a one letter abbreviation for the adduct. Multiple UMP adducts are seen (dashed line). Reactions were performed (i) in the standard Hepes/KCl buffer, (ii) in the absence of buffer (lane marked none), (iii) in the presence of the indicated concentrations (in mM) of Hepes (pH 7.6) alone, or (iv) with 100 mM Na-phosphate (pH 7.6). AMP and UMP quencher concentrations were 500 mM; pyridine was 100 mM. 84S RNAs lacking (−) the aryl azide contained a 2′-amine group at position 84. For clarity, identical control reactions (lanes 3 and 4) were loaded twice on the gel.

irradiation of the 84S RNA, but not the underivatized RNA, reproducibly yields a product band of reduced mobility (see arrow in lane 4 of Figure 6). This band shows a concentration-dependent intensity when the RNA is irradiated in the presence of 100, 50, or 25 mM buffered Hepes alone (lanes 6, 7, and 8 in Figure 6). In contrast, the photoadduct is absent in samples photolyzed in water alone or in 100 mM non-nucleophilic sodium phosphate buffer (compare lane 6 with the no buffer and Na-phos lanes, 5 and 9, in Figure 6). These experiments strongly support assignment of the low mobility band as reporting a direct phenyl azide−Hepes diamine photoadduct.

Photolysis in the presence of AMP in both Hepes/KCl and Na-phosphate buffers consistently yields a well resolved low mobility product (Figure 6, lanes 10 and 15). As expected, formation of the AMP−RNA adduct competes with and decreases the relative intensity of the Hepes adduct (compare Hepes band in lane 4 with lane 10). Interestingly, photolysis of the 84S RNA in the presence of UMP yields several bands of reduced mobility (Figure 6, lanes 11 and 16), suggesting adduct formation with UMP resolves to multiple photoproducts.

UV irradiation in the presence of 100 mM pyridine yields a band that migrates just above that of the aryl azide-derivatized 84S RNA starting material (Figure 6, arrow in lane 12). The pyridine-dependent band completely replaces the Hepes adduct (compare pyridine and Hepes adducts in lanes 12 and 4, in Figure 6), consistent with formation of a direct pyridine adduct. Because the pyridine band is just barely resolved from the starting material, there also exists the possibility that the new band reports conversion of the ketenimine to the azepinone (as discussed below and illustrated in Scheme 1).

The AMP, UMP, Hepes, and putative pyridine adducts each have relative mobilities that correlate with their molecular masses (Figure 6). Importantly, resolution of these photoproducts emphasizes that the photoactivated species forms physical adducts with nucleotide monophosphates and with the Hepes component of our standard reaction buffer. The reactive intermediate is also, at least, intercepted by pyridine.

Photochemistry of 3-Hydroxyphenyl Azide. Thus far, we have shown that photoactivation of the RNA-tethered 3-hydroxyphenyl azide group yields RNA cross-links and nucleotide adducts consistent with a ketenimine or ketenimine-derived intermediate. We then sought to visualize directly the species responsible for cross-linking and to place limits on the lifetime

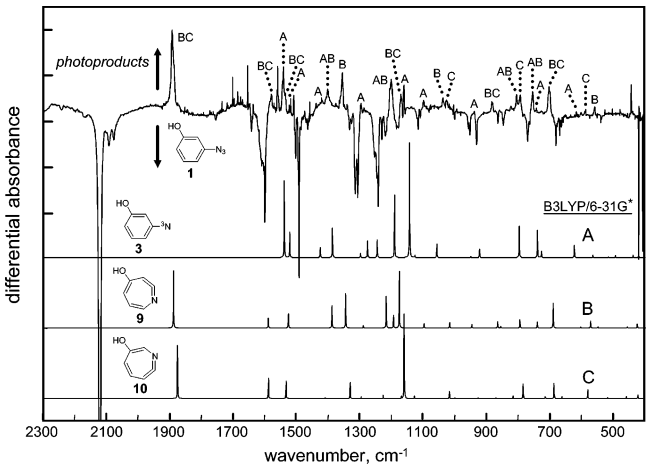

Figure 7. Differential IR spectrum produced by photolysis of 3-hydroxylphenyl azide (**1**) in an argon matrix. Irradiation was performed at 254 nm for 2 min. In the experimental spectrum (top), the primary photoproducts and consumption of the 3-hydroxyphenyl azide starting material are reported as positive and negative peaks, respectively. Compounds **3** (A), **9** (B), and **10** (C) are referenced to their calculated[29] spectra (lower panels).

of the photoactivated reaction intermediate in aqueous, buffered solution. To this end, we explored the photochemistry of free 3-hydroxyphenyl azide using tools of matrix isolation spectroscopy, laser flash photolysis, and computational chemistry. Free 3-hydroxyphenyl azide lacks the *para* amido linkage that tethers the aryl azide to the RNA backbone in the 84D duplex (Figure 2A). However, because *para*-carbonyl substituents have little influence on the intrinsic kinetic and spectroscopic properties of singlet and triplet aryl nitrenes,[20] the simpler 3-hydroxyphenyl azide is a good model for the RNA-tethered aryl azide.

Argon Matrix Studies. One way to observe otherwise transient and highly reactive photoproducts is to perform experiments in a (solid) argon matrix. In this matrix, there is little diffusion and only primary photoproducts or their unimolecular rearrangement products are observed. Photolysis of 3-hydroxyphenyl azide (**1**) in an argon matrix (254 nm, ∼16 K) for 30−120 s led to the rapid disappearance of the infrared (IR) spectra of the azide starting material (Figure 7, top; negative peaks correspond to azide depletion). 3-Hydroxyphenyl azide photolysis is expected initially to produce a metastable singlet nitrene (**2**, Figure 1) which can either intersystem cross to the ground-state triplet nitrene (**3**), or rearrange on the singlet surface

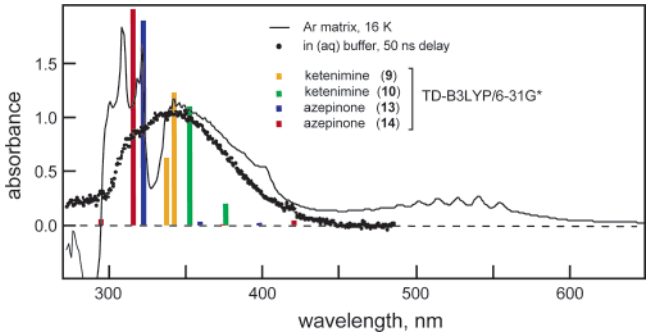

Figure 8. Differential UV−vis spectra of 3-hydroxyphenyl azide (**1**). Spectra are shown for photolysis in an argon matrix (254 nm, 2 min) at 16 K (solid line) and in aqueous solution (355 nm, 50 ns delay) containing 50 mM Hepes (pH 7.6), 50 mM KCl at 22 °C (experimental points shown as solid circles). Bars indicate simulated low energy transitions for ketenimine (**9**/**10**) and azepinone (**13**/**14**) species, calculated at the TD-B3LYP/6-31G* level.[29,32]

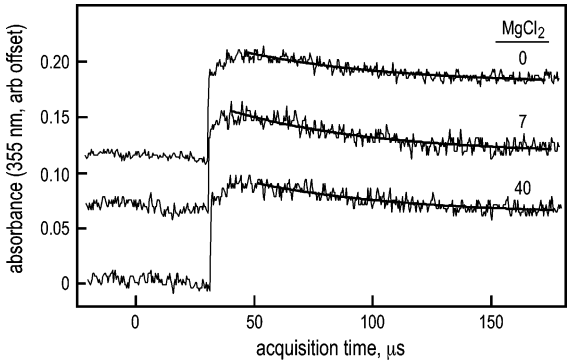

Figure 9. Lifetime of the photoactivated species is independent of $MgCl_2$ concentration. Transient absorbance was monitored at 355 nm following laser flash photolysis (266 nm) of 3-hydroxyphenyl azide (**1**) in 50 mM Hepes (pH 7.6), 50 mM KCl. Decay half-lives at 0, 7, and 40 mM $MgCl_2$ are identical (at 62 ± 3 μs) within error. Curves are shown with arbitrary offsets.

to produce first azirines **7**/**8** and then the ketenimines **9**/**10**.[7,8,18,20] Calculated[29] vibrational frequencies for compounds **3**, **9**, and **10** reproduce the experimental IR spectra well (compare calculated transitions A, B & C with the experimental spectra in Figure 7).

The product spectrum contained a strong band at 1891 cm^{-1}, indicative of the N═C═C stretching frequency of the ketenimine,[10] and a medium intensity band at 1539 cm^{-1}, characteristic of the C═C stretch of triplet nitrene **3**[30] (see positive peaks in Figure 7). Prominent bands attributed to the ring expanded ketenimine isomers include bands at 1578, 1532, and 1167 cm^{-1}, corresponding to vibrational modes for C═C and O−H stretches. Overall inspection of the product IR spectrum suggests roughly equal amounts of nitrene **3**, and ring expanded isomers **9** and **10** are present in the argon matrix.

Having assigned the initial photoproducts produced upon photolysis of 3-hydroxyphenyl azide (**1**) by IR spectroscopy, we then visualized these products in the UV−vis region, the spectroscopic technique which we will later use to interpret time-resolved experiments. Photolysis of **1** in the argon matrix (2 min at 254 nm) resulted in the disappearance of the azide and the formation of new bands at 311, 324, 350, 390, 411, and 556 nm (solid line in Figure 8). The bands at 311, 324, and 411 nm are relatively sharp and are characteristic of the triplet nitrene.[20] The broad band at 556 also reports the triplet[20] and nontrivially contains an ordered vibrational progression of 480 cm^{-1}. This progression is not typical of triplet aryl nitrenes, and the low-frequency excited-state mode responsible for these transitions cannot be assigned at this time.

The broad absorption at 350 nm is exactly that expected for a ketenimine species, based on laser flash photolysis studies of numerous substituted phenyl azides,[20] and is likely due to a mixture of compounds **9** and **10**. Moreover, the UV−vis spectra recorded in glassy matrixes (2-methyltetrahydrofuran or 3-methylpentane, not shown) are similar to that obtained in the argon matrix (Figure 8) with one major distinction. The broad absorption at 350 nm seen in the argon matrix is largely absent in spectra obtained using glassy matrixes. Argon matrixes accept heat less well than do glassy matrixes, and thus, the 350 nm band reflects a species produced by a unimolecular rearrangement[31] which surmounts a small but finite barrier, as expected for ketenimine formation. Finally, simulations of the UV−vis spectra (calculated at the TD-B3LYP/6-31G* level[29,32]) predict low energy ketenimine transitions for both **9** and **10** to occur exactly in the 350 nm region (see yellow and green bars in Figure 8). In sum, these argon matrix studies emphasize formation of the ketenimine as the major initial intermediate produced upon photolysis of 3-hydroxyphenyl azide.

Laser Flash Photolysis Studies. We then studied the transient photoproducts produced upon pulsed photolysis (266 or 308 nm) of 3-hydroxyphenyl azide (**1**) under aqueous solution conditions identical to those used in the RNA cross-linking studies. There is no difference in the transient absorption spectrum (λ_{max} = 355 nm) recorded immediately after the laser pulse (a 50 ns delay, see closed circles in Figure 8) versus that obtained following a 1 μs delay (data not shown). The observed transient spectrum is also identical for experiments performed with air versus nitrogen saturated solutions. Because triplet nitrenes are quenched by molecular oxygen, these data indicate that the transient species seen in aqueous solution is not the triplet nitrene, consistent with the cross-linking experiments discussed above and with extensive prior spectroscopic work.[8,20] The transient lifetime is also independent of phenyl azide concentrations spanning 10^{-5}−10^{-3} M, suggesting decay reflects a unimolecular or pseudo-first-order process and is not due to reaction of the transient with a second equivalent of azide under these experimental conditions.

We determined the time constant for decay of the transient species by pulsed irradiation of a solution of 3-hydroxyphenyl azide and observing the change in absorbance at 350 nm (Figure 9). The strongly absorbing transient species forms within the 20 ns duration of the laser pulse and, under our standard reaction conditions, decays with a time constant of 62 μs (Figure 9). The rate of transient decay is unaffected by $MgCl_2$ concentrations spanning 0−40 mM (Figure 9). In contrast, the transient spectrum observed in pure water is identical to that observed in Hepes buffer (solid circles in Figure 8), but the lifetime of the transient in water is greater than several hundred microseconds (data not shown). These observations are inconsistent with a nitrenium ion carrier of transient absorption as this species decays in a few microseconds in water.[9,22,23]

(29) Frisch, M. J.; et al. *Gaussian 98*, revision A.7; Gaussian, Inc.: Pittsburgh, PA, 1998.
(30) Hayes, J. C.; Sheridan, R. S. *J. Am. Chem. Soc.* **1990**, *112*, 5879−5881.
(31) LeBlanc, B. F.; Sheridan, R. S. *J. Am. Chem. Soc.* **1988**, *110*, 7250−7252.
(32) Hill, B. T.; Platz, M. S. *Phys. Chem. Chem. Phys.* **2003**, *5*, 1051−1058.

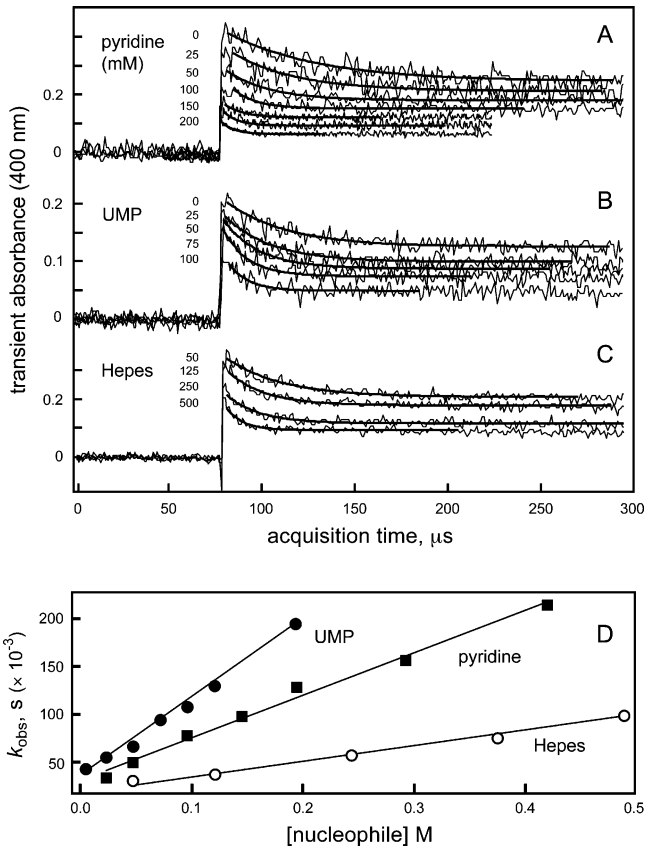

Figure 10. Reaction of the activated species produced upon photolysis of 3-hydroxyphenyl azide with pyridine, UMP, and Hepes (pH 7.6). Solid lines in A, B, and C represent best fits to a single exponential. (D) Second-order rate constants for reaction of UMP, pyridine, and Hepes at pH 7.6 with the transient produced by photolysis of 3-hydroxyphenyl azide. Rate constants for reaction with UMP, pyridine, and Hepes are 7.4×10^5, 4.4×10^5, and 1.6×10^5 M^{-1} s^{-1}, respectively.

Importantly, the transient selectively decays in the presence of Hepes buffer but not in pure water. Similarly, cross-linking experiments indicate that photoactivation of RNA-tethered 3-hydroxyphenyl azide yields a distinctive adduct in the presence of Hepes but not in water or phosphate buffer (see Hepes, none, and Na-phos lanes in Figure 6). These data strongly imply that the photoactivated species forms an adduct with the Hepes diamine. Formation of a direct adduct is reasonable because ketenimines **9**/**10** or ketenimine-derived isomerization products (see below) are strong electrophiles presumably capable of reacting with the tertiary amine groups in the Hepes diamine.

Increasing the Hepes diamine concentration causes the transient species to decay more rapidly (Figure 10C). The observed pseudo-first-order rate constant for disappearance of the transient is linearly dependent on the Hepes concentration. Buffered Hepes diamine (pH 7.6) reacts with an absolute second-order rate constant rate constant of 1.6×10^5 M^{-1} s^{-1} (Figure 10D). The transient does not decay to baseline at 350 or 400 nm, consistent with reaction of the diamine to form a product with lower (but non-zero) absorbance than the photogenerated species.

Pyridine and UMP also both quench formation of the cross-strand cross-link (Figures 4B,C and 5C, respectively) and react with the transient species in a concentration-dependent manner (Figure 10A,B). Pyridine and UMP react with the photogenerated transient species with absolute rate constants of 4.8×10^5 and 4.4×10^5 M^{-1} s^{-1}, respectively (Figure 10D). Laser flash photolysis experiments could not be performed with AMP due to the large absorption of this compound at 308 nm, the wavelength of the exciting laser pulse. Importantly, DMSO, which does not quench cross-link formation (Figure 4A), also does not shorten the lifetime of the transient even at concentrations as high as 500 mM (data not shown). These data support the interpretation that the carrier of the transient spectra (Figures 8 and 10) is the species responsible for formation of RNA cross-links (Figure 3B,C) and for forming physical adducts with Hepes and UMP (Figure 6).

Discussion

Aryl azide photochemistry is complex and can produce reactive species with widely varying chemical selectivities and lifetimes (Figure 1). We were concerned primarily with the usefulness of an RNA-tethered 3-hydroxyphenyl azide group for mapping structures and dynamic intermediates in RNA folding reactions.

Ketenimine and Azepinone Candidates for the Photoactivated Species. Our data are certainly consistent with the transient absorption reflecting a mixture of ketenimines **9**/**10** (Figure 1). The transient spectra and lifetimes are consistent with those expected for these intermediates[20] and with matrix spectroscopy (Figure 7) and density functional theoretical calculations that predict that **9**/**10** will absorb in this region in solution.

Because the aryl azide studied in this work contains a hydroxyl group, an additional possibility is that the ketenimine products could undergo prototropic rearrangement to the corresponding azepinones (**13**/**14**; Scheme 1). This enol-keto isomerization has been documented for *para*-hydroxy-substituted aryl azides in matrix studies.[16] Although the hydroxy-substituted ketenimines **9**/**10** of this work could, in principle, undergo prototropic rearrangement in argon, we did not detect the expected azepinones in our matrix study (Figure 7). Modest support for some azepinone formation comes from density functional theory calculations (see blue and red bars in Figure 8) that suggest the small shoulder at 315 nm, detected in aqueous solution, may report the presence of azepinones.

If the azepinone is the carrier of the signal, it is formally possible that Hepes-, pyridine-, and UMP-mediated decay reflects, in part, base-catalyzed isomerization of the hydroxy-substituted ketenimines (**9**/**10**) to the keto-ketenimines (**9k**/**10k**) or azepinones (**13**/**14**; Scheme 1). The parent ketenimine reacts with pyridine (at 4.8×10^5 M^{-1} s^{-1} in dichloromethane) to form an intensely absorbing long-lived ylide;[17] whereas, the transient produced upon flash photolysis of **1** in Hepes buffer or dichloromethane does not react with pyridine to form an ylide that absorbs in the visible region of the spectrum (Figure 10 and data not shown). To explain these data, either base-catalyzed isomerization of the hydroxyketenimine would have to be more rapid than ylide formation or the hydroxy-substituted ylide must undergo further prototropic rearrangement to form an adduct which lacks a distinctive chromophore in the visible.

The most economical interpretation of the data is that hydroxy-ketenimine **9**/**10** is the carrier of the transient spectrum detected in aqueous buffer and that it reacts with nucleotides (Figure 11) to form adducts. The data are also consistent with azepinones **13**/**14** as partial carriers of the transient spectra and

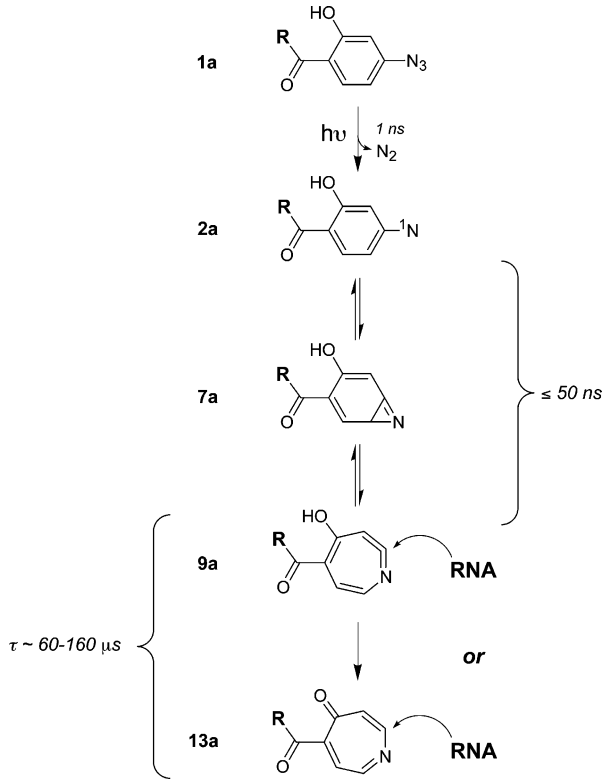

Figure 11. 3-Hydroxyphenyl azide photolysis chemistry yielding covalent adducts with RNA. Ring expansion to the ketenimine is complete prior to detection in flash photolysis experiments and must occur in less than 50 ns. For clarity, only single ring isomers of the ketenimine (**9a**) and azepinone (**13a**) intermediates are shown. The lifetime of the photoactivated species **9a**/**13a** is governed primarily by reaction with the aqueous Hepes buffer (50 mM) and would be different under other buffer conditions.

the cross linking species (Figure 11). In either case, the reactive species is a strong electrophile capable of reacting broadly with all four RNA monomers (Figures 5 and 6 and see ref 3).

Overall Pathway for Photoinduced Cross-Linking with 3-Hydroxyphenyl Azide. The initial product of aryl azide irradiation is the singlet nitrene (**2** and **2a**; Figures 1 and 11).[8] The reactive species is not quenched by dimethyl sulfoxide or acrylamide (Figure 4A), providing strong chemical evidence that, as expected,[11,20] the ultimate reactive intermediate is not the initially produced singlet nitrene. Similarly, cross-linking is independent of the concentration of the 84D duplex, which rules out cross-link formation via triplet nitrene dimers (see **5** in Figure 1). Both argon matrix (Figure 7) and solution phase (Figure 8) studies indicate that the expected ketenimine species (**9**/**10** or **9a**/**10a**) and potentially a smaller amount of the corresponding azepinones (**13a**/**14a**) are present following photolysis of 3-hydroxyphenyl azide.

Consistent with the reactivity expected for a strong electrophile, the cross-linking species is intercepted by pyridine, nucleotide monophosphate, and Hepes nucleophiles (Figures 4B,C, 5, and 6). Together with prior work,[7−9,16] these results argue strongly for a mechanism in which photolysis of 3-hydroxylphenyl azide yields RNA cross-links via the simplified scheme shown in Figure 11. Irradiation of the RNA-tethered 3-hydroxyphenyl azide (**1a**) yields the singlet nitrene (**2a**),[8] which undergoes rapid ring expansion to form the ketenimine (**9a**) and, possibly, azepinone (**13a**) electrophiles. The electrophilic species is sufficiently reactive toward nucleophiles that (i) AMP, UMP, and GMP exhibit similar quenching profiles and (ii) all four ribonucleotides form intramolecular cross-links with photolyzed aryl azides in large RNAs.[2,3]

Lifetime of the Reactive Electrophile. We estimate a lifetime for the reactive species in aqueous solution by three independent approaches. First, we followed the decay of free 3-hydroxyphenyl azide as a function of $MgCl_2$ concentration by photolyzing the aryl azide and monitoring absorbance at 355 nm (Figure 9). The transient species decays with a time constant of 62 μs, independent of Mg^{2+} or chloride ion concentration. Second, we determined a second-order rate constant of 1.6×10^5 M^{-1} s^{-1} for reaction of the photoactivated species with buffered (pH 7.6) Hepes diamine (Figure 10C,D). At the 50 mM Hepes concentration used in our standard conditions, the time constant for decay of the photoactivated species is $1/[(1.6 \times 10^5\ M^{-1}\ s^{-1}) \times (0.050\ M)]$ or 88 μs. This value is in excellent agreement with that obtained by monitoring individual transients directly (Figure 9). Both of these estimates for decay of the reactive intermediate were obtained using free 3-hydroxyphenyl azide which resembles closely, but is not identical to, the RNA-tethered phenyl azide (Figure 2A) used in the RNA photo-cross-linking studies (Figure 3 and ref 3).

Third, a superior calculation makes use of our pyridine quenching experiments to define the reactive lifetime specifically under the experimental conditions used for RNA-tethered photo-cross-linking. The transient species generated upon photolysis of 3-hydroxyphenyl azide reacts with pyridine with a rate constant of 4.4×10^5 M^{-1} s^{-1} under our standard reaction conditions (Figure 10A,D). Pyridine intercepts one-half of the 84D cross-strand RNA cross-link at a concentration of 14 mM (Figure 4C); at 14 mM pyridine, the rate of trapping is therefore 6.2×10^{-3} s^{-1}. This is the rate at which one-half of the photoactivated intermediate is intercepted by pyridine and is also the total rate at which the reactive intermediate is consumed by labeling, plus reaction with solvent and Hepes, and conversion to other unreactive species. Thus, the time constant for decay of the photoactivated species under our, Hepes buffered, aqueous reaction conditions is $1/(6.2 \times 10^{-3}\ s^{-1})$ or 160 μs. This decay time constant is within a factor of 3 for time constants obtained for the ketenimine-derived reactive intermediate produced upon photolysis of *free* 3-hydroxyphenyl azide (62−88 μs) and provides additional support that 3-hydroxyphenyl azide is a good model for the RNA-tethered phenyl azide.

Lifetime of the Labeling Intermediate Compared with that of RNA Folding Reactions. The lifetime of the photoactivated intermediate (60−160 μs) is substantially shorter than almost all known RNA folding events (reviewed in Figure 12). The only RNA folding event whose time constant is comparable to that of photoactivated 3-hydroxyphenyl azide is simple hairpin loop formation. This is not a significant concern as long as experiments are initiated in the presence of modest monovalent ion concentrations because hairpin loop structures will have already formed.[33] Rate constants for structural transitions likely to dominate RNA folding and RNP assembly reactions, including folding of large loops, formation of local tertiary structure, and conformational switches, are 1 to 4 orders of magnitude slower than the ketenimine-derived lifetime (Figure 12).

Support for a short lifetime, that eliminates the ability of the photoactivated species to sample multiple RNA structures, is

(33) Chamberlin, S. I.; Weeks, K. M. *Biochemistry* **2003**, *42*, 901−909.

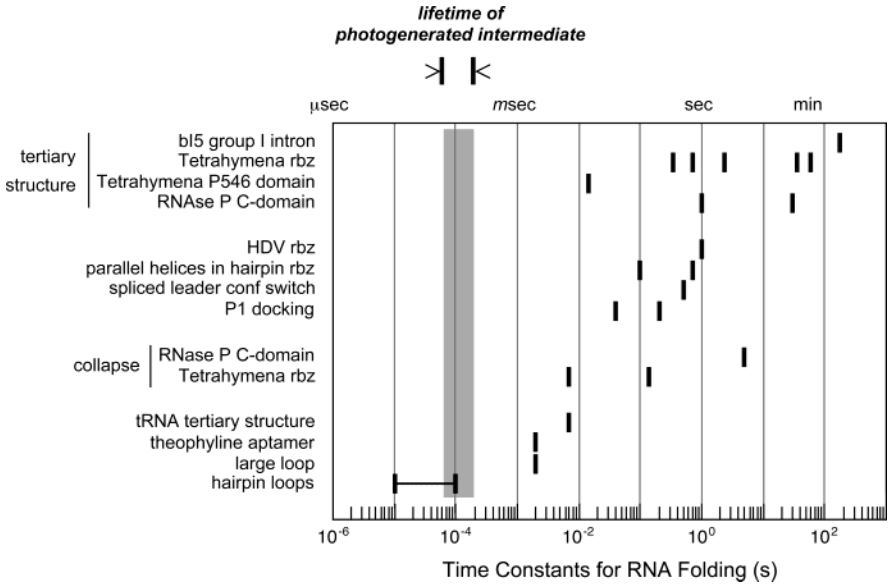

Figure 12. Comparison of the lifetime for photoactivated 3-hydroxyphenyl azide with time constants for RNA folding events. References for RNA folding time constants are the following: hairpin loops, large loops, and tRNA tertiary structure (ref 36 and references therein); theophylline aptamer active site;[37] collapse of the RNase P C-domain and Tetrahymena ribozyme (rbz);[38] P1 docking in the Tetrahymena rbz;[39] spliced leader conformational switch;[40] hairpin rbz;[41] fast folding HDV rbz;[42] RNase P C-domain;[43] Tetrahymena P546 domain;[44] Tetrahymena rbz;[45] and bI5 intron.[46]

supported in an independent way by the lack of intramolecular cross-linking with the single stranded 84S RNA. No *intra*-molecular cross-links form even though the single stranded RNA does form an adduct with AMP, which shows that the single stranded RNA is competent for cross-linking (Figure 5). Thus, the activated species is not sufficiently long-lived to over-report transient looped RNA conformations in this unstructured oligonucleotide.

Total cross-linking efficiencies using RNA-tethered 3-hydroxyphenyl azide are 5−7% for cross-links involving proximal structures and roughly 0% for nonadjacent structures (Figures 3 and 5 and ref 3). This mechanistic study emphasizes that low, but reproducible, cross-linking efficiencies are desirable. Upon photoactivation, the ketenimine or azepinone reactive intermediate (Figure 11) either reacts with RNA (or protein) or is quenched by reaction with an alternate nucleophile, the Hepes diamine. Paradoxically, very efficient cross-linking is likely to reflect an undesirable long lifetime that allows the photoactivated species to persist in solution and form cross-links with infrequently populated RNA conformations.

In sum, RNA-tethered photo-cross-linking with 3-hydroxyphenyl azide involves a photoactivated intermediate, likely a ketenimine or azepinone, that reacts broadly with RNA nucleotides and other nucleophiles. The lifetime of the reactive intermediate is short compared with RNA folding events. Photo-cross-linking with 3-hydroxyphenyl azide in Hepes buffer can be used with confidence to map structural neighbors in dynamic RNA molecules.

Experimental Section

RNAs. All reactions were carried out in 50 mM Hepes (pH 7.6), 50 mM KCl, and $MgCl_2$ at 22 °C in amber tubes with the overhead lights off, except for the experiments using alternate buffers described in Figure 6. Comparable cross-linking results were obtained under air or with 80% nitrogen saturated solutions. The 33 nt 84S oligoribonucleotide (Figure 2) was synthesized containing a unique 2′-amino uridine at position 84 (Dharmacon Research) and 5′-end labeled using T4 polynucleotide kinase (NEB) and γ-[^{32}P]-ATP. The crude 5′-end labeled RNA was derivatized with the 3-hydroxylphenyl azide cross-linking group via a 2′-amido linkage by three sequential treatments with 50 mM *N*-hydroxysuccinimidyl-4-azidosalicylic acid (Pierce Scientific) in 100 mM Hepes (pH 7.6), 50% v/v formamide (22 °C, 1 h, 60−110 μL vol's). Reactions were microcentrifuged after each modification step (15 s; 14 000 rpm) to remove insoluble succinimidyl ester products, and the supernatant was transferred to a new tube for subsequent modification reactions. Excess reagent was removed by G-50 size exclusion chromatography, and after ethanol precipitation, the oligonucleotide was purified by denaturing gel electrophoresis (20% polyacrylamide gels, 7 M urea, 90 mM Tris-borate; 0.75 mm × 31 cm × 38.5 cm; 70 W for 4 h). RNAs were recovered from the gel by passive elution into 500 mM Na-acetate (pH 6), 1 mM EDTA, precipitated with ethanol, and stored in water at −20 °C. Duplex RNAs were assembled by annealing 4 nM each aryl azide-modified 33 nt and complementary 32 nt oligoribonucleotides by heating to 90 °C for 3 min, cooling to 25 °C over 20 min, and incubating in reaction buffer at 22 °C for 5−20 min. The 84S single stranded RNA was prepared by omitting the 32 nt complement but otherwise treated identically to the duplex RNA.

Cross-Linking Reactions. Duplex and single stranded RNAs (0.4 nM) were irradiated with polystyrene filtered UV−B light from a midrange Hg lamp (UVP Inc., λ_{max} 312 nm, $I_{90\%}$ 285−345 nm, ~3 W at surface). Cross-linking reactions (10 μL, 4.4 cm from the light source, 1 or 10 min) were quenched by the addition of excess dithiothreitol (DTT) and 80% formamide containing 45 mM tris-borate, 50 mM EDTA, and tracking dyes. Control experiments demonstrated that DTT reduces free 3-hydroxyphenyl azide to the corresponding aniline in the dark within seconds. Cross-linking products were resolved on 20% denaturing polyacrylamide gels, and bands were quantified using a Phosphorimager (Molecular Dynamics). The position of the cross-strand cross-link (Figure 2C,D) was mapped by alkaline hydrolysis, as described previously.[3]

Quenchers. Pyridine, DMSO, and acrylamide (as a 29:1 ratio of acrylamide:bisacrylamide) were ≥99% pure and were diluted in water. The AMP free acid (USB) was dissolved in sodium phosphate and the pH adjusted to 7.5 with NaOH. UMP (Sigma) and GMP (Sigma) were dissolved in water, and the pH of GMP was adjusted to 7.5 with HCl; the pH of UMP was 7.5 without adjustment. Concentrations of AMP,

UMP, and GMP were determined by UV spectrometry using extinction coefficients of 15.4, 10.0, and 13.7 mM^{-1} cm^{-1}, respectively.

Laser Flash Photolysis Studies. Samples (1 mL, 22 °C) were typically prepared with an absorbance of ~1 at the irradiation wavelength, either 254 or 308 nm. Concentration-dependent experiments were performed over 10^{-5} to 10^{-3} M 3-hydroxyphenyl azide. The laser flash photolysis apparatus[34,35] used either a Spectra Physics LAB-150-10 (~5 ns) water-cooled laser, configured to supply 266 nm radiation, or a Lambda Physik LPX-100 excimer laser (308 nm, 120 mL, 10 ns). The current design of the flash photolysis instrument has been described in detail[35] and uses the LabView graphic programming language, facilitating instrument operation and experiment optimization. The instrument features dual ports, one with a slit and photomultiplier for kinetic measurements and the other with a flat field and digital ICCD camera for spectroscopic measurements. Data were analyzed[34] using the Igor Pro package (Wavemetrics); all transients were well fit as single exponentials.

Matrix Isolation Spectroscopy. 3-Hydroxyphenyl azide (**1**) was deposited by sublimation onto either CsI (IR) or CaF_2 (UV−vis) windows cooled to 16 K using a closed-cycle cryogenic apparatus (Air Products) in the presence of a continuous stream of argon. Argon matrixes were photolyzed using a Rayonet reactor with variable wavelength bulbs. Infrared and UV−vis spectra were recorded with Perkin-Elmer FTIR 2000 (2 cm^{-1} resolution) and Perkin-Elmer Lambda 6 spectrometers, respectively.

Model Spectra Calculations. Density functional theory calculations were performed using the Gaussian 98 software package.[29] The geometries of potential 3-hydroxyphenyl azide photoproducts were fully optimized at the B3LYP level using the 6-31G* basis set, as outlined previously.[32] Unrestricted (U)B3LYP methods were used for the triplet state. B3LYP/6-31G* vibrational frequencies were scaled by 0.9614 for comparison to experimental IR spectra.

Acknowledgment. This work was supported by grants from the NIH (GM56222 to K.M.W.) and NSF (CHE-9613861 to M.S.P.). B.T.H. gratefully acknowledges support of an Ohio State University Postdoctoral Fellowship. We thank Malcolm Forbes and Robert McClelland for helpful discussions.

JA035743+

(34) Gristan, N. P.; Zhai, H. B.; Yuzawa, T.; Karweik, D.; Brooke, J.; Platz, M. S. *J. Phys. Chem. A* **1997**, *101*, 2833−2840.
(35) Martin, C. B.; Shi, X.; Tsao, M.-L.; Karweik, D.; Brooke, J.; Hadad, C. M.; Platz, M. S. *J. Phys. Chem. B* **2002**, *106*, 10263−10271.
(36) Crothers, D. M.; Cole, P. E.; Hilbers, C. W.; Shulman, R. G. *J. Mol. Biol.* **1974**, *87*, 63−88.
(37) Jucker, F. M.; Phillips, R. M.; McCallum, S. A.; Pardi, A. *Biochemistry* **2003**, *42*, 2560−2567.
(38) (a) Fang, X.-W.; Thiyagarajan, P.; Sosnick, T. R.; Pan, T. *Proc. Natl. Acad. Sci. U.S.A.* **2002**, *99*, 8518−8523. (b) Russell, R.; Millett, I. S.; Tate, M. W.; Kwok, L. W.; Nakatani, B.; Gruner, S. M.; Mochrie, S. G. J.; Pande, V.; Doniach, S.; Herschlag, D.; Pollack, L. *Proc. Natl. Acad. Sci. U.S.A.* **2002**, *99*, 4266−4271.
(39) (a) Bevilacqua, P. C.; Kierzek, R.; Johnson, K. A.; Turner, D. H. *Science* **1992**, *258*, 1355−1358. (b) Narlikar, G. J.; Bartley, L. E.; Khosla, M.; Herschlag, D. *Biochemistry* **1999**, *39*, 14192−14204.
(40) LeCuyer, K. A.; Crothers, D. M. *Proc. Natl. Acad. Sci. U.S.A.* **1994**, *91*, 3373−3377.
(41) Zhuang, X.; Kim, H.; Pereira, M. J.; Babcock, H. P.; Walter, N. G.; Chu, S. *Science* **2002**, *296*, 1473−1476.
(42) Chadalavada, D. M.; Senchak, S. E.; Bevilacqua, P. C. *J. Mol. Biol.* **2002**, *317*, 559−575.
(43) Fang, X.-W.; Pan, T.; Sosnick, T. R. *Nat. Struct. Biol.* **1999**, *6*, 1091−1095.
(44) Deras, M. L.; Brenowitz, M.; Ralston, C. Y.; Chance, M. R.; Woodson, S. A. *Biochemistry* **2000**, *39*, 10975−10985.
(45) (a) Zarrinkar, P. P.; Williamson, J. R. *Science* **1994**, *265*, 918−924. (b) Sclavi, B.; Sullivan, M.; Chance, M. R.; Brenowitz, M.; Woodson, S. A. *Science* **1998**, *279*, 1940−1943.
(46) (a) Weeks, K. M.; Cech, T. R. *Science* **1996**, *271*, 345−348. (b) Webb, A. E.; Rose, M. A.; Westhof, E.; Weeks, K. M. *J. Mol. Biol.* **2001**, *309*, 1087−1100.